Mitigating Correlation Problems in Turbo Decoders

Ronald Garzón-Bohórquez, Rami Klaimi, Charbel Abdel Nour, and Catherine Douillard

IMT Atlantique, CNRS UMR 6285 Lab-STICC Brest, France
Email: {ronald.garzonbohorquez, rami.klaimi, charbel.abdelnour, catherine.douillard}@imt-atlantique.fr

Abstract—In this paper, new interleaver design criteria for turbo codes are proposed, targeting the reduction of the correlation between component decoders. To go beyond the already known correlation girth maximization, we propose several additional criteria that limit the impact of short correlation cycles and increase code diversity. Two application examples are elaborated, targeting an 8-state binary turbo code and a non-binary turbo code defined over GF(64). The proposed design criteria are shown to improve the error correcting performance of the code, especially in the error floor region.

Index Terms—Turbo codes, correlation in decoding, interleaving, asymptotic performance.

I. INTRODUCTION

With the upcoming TeraHertz communications, a new generation of channel coding technology has to be developed, able to offer higher data throughputs and a higher reliability. To this end, an issue still to be addressed is the improvement of the asymptotic performance of capacity approaching codes such as turbo codes (TCs) or low-density parity-check (LDPC) codes, especially at high coding rates. As far as TCs are concerned, significant progress has been made recently to lower the error floor of punctured TCs through the design of puncture-constrained interleavers [1]. However, in some cases, it can be observed that the resulting codes are not able to approach the asymptotic bound predicted by their Hamming distance spectrum [1]. A possible reason for such a behaviour is the high correlation between the exchanged information during the iterative process [2], [3]. Very few tools have been proposed to design encoders reducing the introduced correlation among the encoded symbols. In [4], a correlation graph was derived for TCs and designing interleavers that maximizes the length of the shortest cycle in the correlation graph, i.e., the correlation girth, was shown to improve the error correction performance of the TC.

In this study, additionally to the already known correlation girth maximization, we propose new design criteria for the interleaver that impact the number and the nature of the short correlation cycles. The remainder of this paper is structured as follows. In Section II, we start by introducing the considered TC and interleaver structures. Section III describes the correlation graph which is further used to define the interleaver design criteria. The proposed criteria are then presented in Section IV and Section V. In Section VI, they are applied to design interleavers for an 8-state TC using tail-biting $(1, 15/13)_8$ component codes and for a non-binary turbo code (NB-TC) defined over GF(64).

II. CONSIDERED TC AND INTERLEAVER STRUCTURE

The TC structure considered in this study is shown in Fig. 1. The information sequence $\mathbf{d}$ and the corresponding interleaved sequence $\mathbf{d}'$ are encoded by two recursive systematic convolutional (RSC) codes C1 and C2, respectively. In order to obtain high coding rates, the vectors at the output of the TC, data ($\mathbf{d}$), parity 1 ($\mathbf{r_1}$), and parity 2 ($\mathbf{r_2}$), are punctured using periodic puncturing masks.
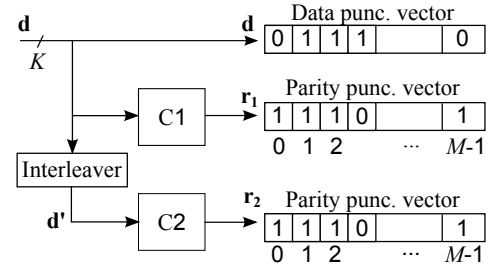

Fig. 1. Considered encoder structure with an example of puncturing mask.

Three of the most popular interleaver families for TCs are the quadratic permutation polynomial (QPP) [5] adopted in LTE [6], the dithered relatively prime (DRP) [7], and the almost-regular permutation (ARP) interleaver [8] adopted in the DVB-RCS/RCS2 [9], [10] and IEEE 802.16 WiMAX [11] standards. As shown in [12], the ARP interleaver can provide the same interleaving properties as the QPP or DRP interleavers, guaranteeing minimum Hamming distance values at least as high as these two families of interleavers. Thus, we only considered the ARP family in our study. However, the proposed design criteria are also valid for the other interleaver families. The ARP function is defined as [4]:

$$\Pi(i) = (P \cdot i + S(i \bmod Q)) \bmod K \quad (1)$$

where $i = 0, ..., K - 1$ denotes the address of the data symbol after interleaving and $\Pi(i)$ represents its corresponding address before interleaving, K being the information block size. P is the regular interleaver period, and S a vector of shifts of length Q.

III. CORRELATION GRAPH FOR TCS

The reduction of correlation is of high importance in iterative decoding processes. For LDPC codes, increasing the length of the shortest correlation cycles in the Tanner graph, i.e. the correlation girth, allows the belief propagation algorithm to improve the error correction of the decoder and to come closer to maximum likelihood performance. In [13], the

authors introduced the progressive edge growth algorithm for the construction of LDPC parity-check matrices to maximize the correlation girth.

In the case of TCs, two types of information exchanges participate to the error correcting process in the turbo decoder: 1) extrinsic information exchange between the two component decoders via the interleaver, 2) local information exchange between neighbouring symbols in each component decoder, due to the convolutional nature of the component codes. These two types of exchanges create some dependency loops between sets of symbols. These dependencies can be represented by cycles in a correlation graph, in the same way as in the Tanner graph for LDPC codes. A possible representation of a correlation graph for a TC is illustrated in Fig. 2 in the case of tail-biting component codes. The vertices of the graph are the K symbols of the information sequence. The connections between neighbouring symbols in $\mathbf{d}$ and in $\mathbf{d'}$ show the dependencies between each symbol and its neighbors with respect to component codes C1 and C2. Each symbol is represented twice, once in natural order in $\mathbf{d}$ and once in interleaved order in $\mathbf{d'}$. The copies of the symbols are connected through K edges, specified by the interleaver where extrinsic information is exchanged. In Fig. 2, these edges are only represented for an example of length-4 cycle in the graph. When applying the Dijkstra algorithm [14] to find the minimum correlation cycle in the graph and to compute the girth, these edges are not counted, since they are only used to join the two copies of each vertex. In the past, only the maximization of the minimum correlation cycle length, i.e. the correlation girth, was addressed to reduce the correlation in the decoding process. In this paper, we propose additional criteria.
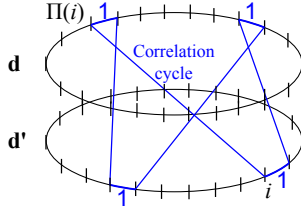

Fig. 2. Example of correlation graph with a length-4 correlation cycle, when using tail-biting RSC component codes.

IV. PROPOSED INTERLEAVER DESIGN CRITERIA TO REDUCE CORRELATION IN TURBO DECODING

The maximum achievable girth depends on the block size and is given by the Moore bound [15]. Therefore, in practice, when the obtained girth is close to this bound, there is little prospect of further gain with girth maximization. However, we have identified three other measurable parameters impacting the correlation of extrinsic information in the decoding process: the multiplicity of the correlation girth (i.e., the number of minimum cycles), the number of transitions between $\mathbf{d}$ and $\mathbf{d'}$ in the minimum correlation cycles, and the number of times a couple of positions in the block participates in multiple instances of short correlation cycles.

A. Multiplicity of the correlation girth

The multiplicity of the correlation girth, $n(g)$, is the total number of minimum correlation cycles. Fig. 3 shows an example of correlation graph with girth $g = 6$ and correlation girth multiplicity $n(g) = 2$. With a large multiplicity of the correlation girth, the decoding errors will more likely propagate along the performed iterations, since erroneous data inside a minimum correlation cycle is more difficult to correct through extrinsic information exchange than erroneous data belonging to only large correlation cycles.

In order to mitigate this correlation problem, the interleaver should be designed to minimize the multiplicity of the correlation girth g, $n(g)$:

$$\text{Select } (Q, P, S) \text{ to } \underset{\text{cycle length} = g}{\text{minimize}} \; n(g) \qquad (2)$$

This criterion can be generalized to a larger set of correlation cycles with short lengths (but greater than the girth).

B. Number of transitions between d and $\mathrm{d'}$ in the minimum correlation cycles

For a given correlation cycle length, the nature of the cycles has an impact on the error correction capability of the decoder. Actually, the correlation in the decoding process can be better mitigated when each information in a short cycle can benefit from a large code diversity, i. e. when parity symbols provided by a high number of different and distant trellis sections participate in the cycle. In long contiguous trellis sections, correlation between the parity bits is created by the convolutional component code and their contribution to the decoding process remains local.

For instance, Fig. 3 shows two length-6 cycles: in the dotted line cycle, each symbol benefits from other symbols coming from three other trellis sections whereas in the other case, each symbol benefits from symbols coming from five single distant trellis sections. The code diversity is therefore higher in the latter case than in the former. This means that cycles with long contiguous trellis sections should be avoided. As for the spatial distance between the different contributing trellis sections, it is guaranteed to be large in practical applications, due to the spreading properties of the interleavers.
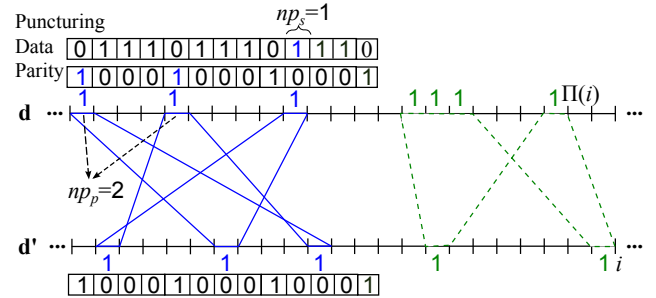

Fig. 3. Example of correlation graph with correlation girth $g = 6$ and multiplicity $n(g) = 2$. Parameter $T_g(\mathbf{d}, \mathbf{d'})$ is equal to 6 for the solid line cycle and to 4 for the dotted line cycle (see Section IV-B).

A proposed design criterion for the interleaver is the maximization of the number of non-contiguous trellis sections

participating in short correlation cycles. Let $T_g(\mathbf{d}, \mathbf{d}')$ be the number of transitions between $\mathbf{d}$ and $\mathbf{d}'$ in the correlation cycles of length g, the interleavers parameters are selected based on:

$$\text{Select } (Q, P, S) \text{ to } \underset{\text{cycle length} = g}{\text{maximize}} \ T_g(\mathbf{d}, \mathbf{d}') \qquad (3)$$

With high values of $T_g(\mathbf{d}, \mathbf{d}')$, more iterations are needed for a particular information symbol to get back to its original position through the information exchanges: autocorrelation is reduced.

Condition (3) is of primary importance for the minimum length correlation cycles but can be generalized to a larger set of correlation cycles with short lengths.

C. Multiplicity of symbol couples in minimum correlation cycles

The last criterion considered in this study is the number of times a couple of symbols participates in different correlation cycles with maximum length $g_{\max}$. This multiplicity parameter is denoted by $m(s, s')$, where s and s' represent any symbol in $\mathbf{d}$ or $\mathbf{d}'$ such that $s \neq s'$. Fig. 4 shows an example of a correlation graph where the couple of symbols (s, s') belongs to four cycles of maximum length 5 (three length-4 and one length-5 cycles): $m(s, s') = 4$ for $g_{\max} = 5$.
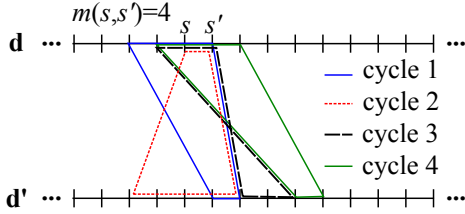

Fig. 4. Example of correlation graph where $m(s, s') = 4$ for $g_{\max} = 5$.

Given that symbols in short correlation cycles are prone to decoding errors, the multiplicity $m(s, s')$ in short cycles should be minimized to reduce the propagation of errors throughout the decoding iterations:

$$\text{Select } (Q, P, S) \text{ to } \underset{\text{cycle length} \leq g_{\max}}{\text{minimize}} \ m(s, s') \qquad (4)$$

V. ADDITIONAL INTERLEAVER DESIGN CRITERION FOR HIGH CODING RATES

In the case of high coding rates, the number of symbols with non-punctured parities in short correlation cycles is inherently limited. Thus, the code diversity experienced by data symbols in these cycles is naturally reduced in comparison to low coding rates. In order to mitigate this detrimental effect, we propose to design the interleaver in such a way to maximize the number of non-punctured parities np_p that participate in short cycles. When using data puncturing, the number of non-punctured systematic bits np_s in short cycles should also be maximized. For illustration purposes, the left-hand correlation graph in Fig. 3 has $np_p = 2$ non-punctured parity symbols and $np_s = 1$ non-punctured systematic symbol.

VI. APPLICATION EXAMPLES

Correlation problems in turbo decoding can be primarily observed for short block sizes. Therefore, we apply the proposed criteria to design ARP interleavers for the encoding of information blocks consisting of approximately 200 bits. Both binary TCs and NB-TCs defined over GF(64) are considered. We adopt the following methodology: first, a set of ARP interleavers is generated for coding rate $R = 1/3$ according to minimum span and correlation girth criteria, as described in [16]. Then, a refinement phase is carried out, using the criteria presented in Section IV. For $R = 2/3$, a periodic puncturing pattern is then designed, taking account of the additional criterion described in Section V. Finally, for the resulting interleavers and puncturing patterns, block error rate (BLER) performance is evaluated by simulation over AWGN channel with QPSK modulation, performing 8 decoding iterations using the scaled Max-Log-MAP algorithm.

A. Binary turbo codes

The interleaver design methodology is first applied to a binary TC using the 8-state tail-biting RSC $(1, 15/13)_8$ component code, for $K = 208$ bits and coding rate $R = 1/3$. Minimum span value $S_{\min} = 15$ and girth $g \geq 6$ are the first constraints considered for the interleaving parameter search. After the refinement phase using the criteria presented in this paper, the winning interleaver (ARP I) is finally selected based on its Hamming distance spectrum. A second interleaver (ARP II) is also selected for comparison purposes: this is the interleaver yielding the best Hamming distance spectrum when using only the minimum span and correlation girth criteria.

Table I provides the interleaver parameters for ARP I and ARP II as well as the values of the new design parameters defined in Section IV. Table II provides the truncated Hamming distance spectra of the corresponding TCs for coding rate $R = 1/3$. Distances and related multiplicities were estimated using the double impulse method with 100 repetitions described in [17]. Both interleavers yield a girth g equal to 6. Table I shows that ARP I has lower values of multiplicities $n(g)$ and $m(s, s')$ and a higher value of $T_g(\mathbf{d}, \mathbf{d}')$ than ARP II. Table II shows that ARP I has a lower minimum distance than ARP II. Nevertheless, the observation of the first terms of the distance spectrum suggests that both codes should display close union bounds.

TABLE I
PARAMETERS P AND S OF ARP I AND ARP II INTERLEAVERS FOR $K = 208$ BITS ($Q = 16$). MINIMUM SPAN $S_{\min} = 15$, GIRTH $g = 6$, CORRESPONDING MULTIPLICITY $n(g)$, MINIMUM NUMBER OF $(\mathbf{d}, \mathbf{d}')$ TRANSITIONS IN A LENGTH-6 CYCLE, $T_g(\mathbf{d}, \mathbf{d}')$, AND MULTIPLICITY OF SYMBOL COUPLES $m(s, s')$ FOR $g_{\max} = g = 6$.

ARP	P	$(S(0), ..., S(15))$	$n(g)$	$T_g(\mathbf{d}, \mathbf{d}')$	$m(s, s')$
I	159	(8, 96, 23, 42, 170, 103, 202, 10, 200, 21, 24, 88, 5, 152, 136, 96)	6	6	2
II	147	(8, 156, 31, 174, 10, 115, 98, 62, 152, 97, 16, 156, 37, 84, 112, 68)	22	4	4

The left-hand curves in Fig. 5 show the impact of interleavers ARP I and ARP II on the BLER performance of the resulting TC for $K=208$ bits and $R=1/3$. As expected, the corresponding truncated union bounds (TUBs) obtained from Table II are very close to each other. Nevertheless, thanks to the correlation reduction, ARP I is able to approach its asymptotic bound 0.25 dB closer than ARP II.
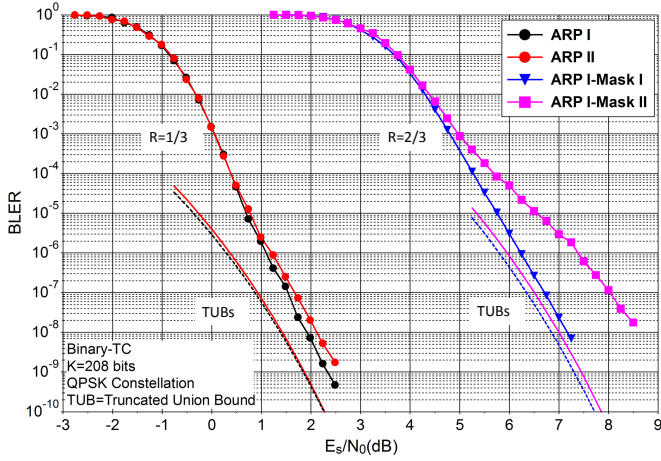

Fig. 5. BLER performance of designed TCs for $K = 208$ bits. Tail-biting RSC$(1, 15/13)_8$ component codes, ARP interleavers defined in Table I and puncturing masks I and II given in Table III. AWGN channel with 8 decoding iterations of the scaled Max-Log-MAP algorithm, $R = 1/3$ and $2/3$, and QPSK modulation.

To verify the proposed criterion for high coding rates, the TC was punctured, keeping optimized interleaver ARP I, to achieve coding rate $R=2/3$. Only periodic puncturing masks were considered in order to make them easy to implement in hardware. The puncturing masks were first selected according to the Hamming distance spectrum of the resulting TC. Then, the final selection was carried out according to the criterion described in Section V. Table III provides two puncturing masks, both yielding minimum Hamming distance 8, as shown in Table IV: mask I was chosen because it maximizes the number of non-punctured parities, np_p, in the shortest correlation cycles while mask II has only punctured parity bits in the shortest correlation cycles.

The right-hand curves in Fig. 5 compare the BLER performance obtained with puncturing masks I and II. The gap between the TUBs of the two resulting TCs for both puncturing masks is less than 0.2 dB whereas the performance gap between the two codes is almost 1.5 dB at BLER $= 10^{-8}$. Thanks to the additional code diversity in short correlation cycles, the code using mask I is able to approach its union bound much closer than the code using mask II.

B. Non-binary turbo codes

The NB-TCs considered in this study were previously investigated in [18] and the structure of the component codes is shown in Fig. 6. Due to decoding complexity reasons, only memory-one component codes were considered, making non-binary decoders more sensitive to correlation problems. In this section, the trellis of the code is defined by coefficients α_1, α_2, and α_3, which are elements of GF(64). These coefficients were chosen to provide the best Euclidean distance spectrum of the convolutional code (see [18]). In the remainder of this paper, $(\alpha_1, \alpha_2, \alpha_3) = (31, 5, 18)$.
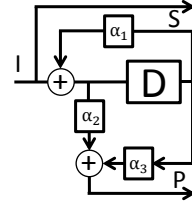

Fig. 6. Non-binary convolutional code structure over GF(q).

The corresponding trellis is fully connected and the shortest error sequences are two trellis sections long. The interleaver design methodology is applied for the encoding of information blocks of $K=30$ symbols in GF(64), corresponding to $K_b = 180$ bits, with coding rate $R = 1/3$. An ARP interleaver is designed following the criteria presented in Section IV. The same methodology as for the binary TC is adopted, except that there is no distance estimation step. Due to the short length of the information blocks, lower values of span and girth are targeted: $S_{min}=5$ and $g \geq 4$. After the refinement phase using the criteria presented in this paper, the winning interleaver (ARP III) is selected based on $n(g)$, $T_g(\mathbf{d}, \mathbf{d}')$ and $m(s, s')$. A second interleaver (ARP IV) is also selected for comparison purposes, which satifies the span and girth constraints, but without undergoing the refinement phase. Table V provides the interleaver parameters defined in (1) for ARP III and ARP IV as well as the values of $n(g)$, $T_g(\mathbf{d}, \mathbf{d}')$ and $m(s, s')$.

The left-hand curves in Fig. 7 compares the impact of interleavers ARP III and ARP IV on the BLER performance of the resulting NB-TC for coding rate $R=1/3$. Similarly to

ARP	Q	P	$(S(0), ..., S(Q-1))$	$n(g)$	$T_g(\mathbf{d}, \mathbf{d}')$	$m(s, s')$
III	3	19	(0,25,14)	2	4	1
IV	5	7	(0,17,3,22,28)	4	4	2

the binary case, thanks to the correlation reduction, ARP III outperforms ARP IV by 0.2 dB at BLER= 10^{-8}.
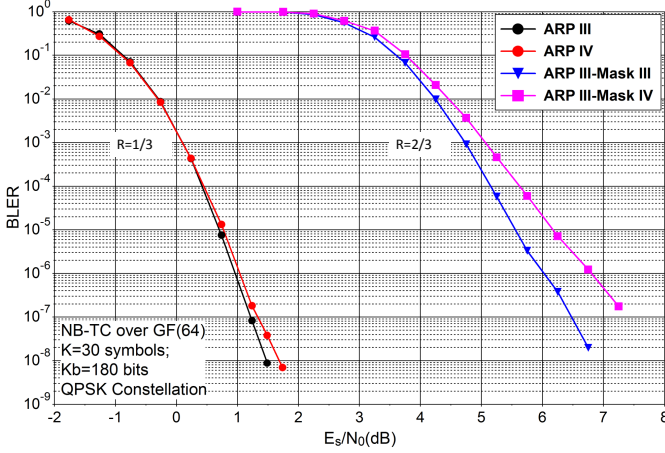

Fig. 7. BLER performance of NB-TCs defined over GF(64) for $K = 30$ symbols ($K_b = 180$ bits). ARP interleavers defined in Table V and puncturing masks III and IV given in Table VI. AWGN channel with 8 decoding iterations of the NB Max-Log-MAP algorithm, $R = 1/3$ and $2/3$, and QPSK modulation.

We finally consider coding rate $R = 2/3$ for the NB-TC. As for the binary case, two puncturing masks are designed for the winning ARP III interleaver, described in Table VI: mask III was chosen because it maximizes the number of non-punctured parities, np_p, in the shortest correlation cycles while mask IV has only punctured parity bits in the shortest correlation cycles.

TABLE VI
PUNCTURING MASKS OPTIMIZED FOR ARP III (NB-TC), $K = 30$
SYMBOLS IN GF(64) ($K_b = 180$ BITS) AND $R = 2/3$. THE PUNCTURING
PERIOD IS $M = 10$, np_s AND np_p ARE THE MINIMUM NUMBER OF
NON-PUNCTURED SYSTEMATIC AND PARITY SYMBOLS IN MINIMUM
CORRELATION CYCLES.

Puncturing mask	Systematic $\mathbf{d}$	Parity $\mathbf{r_1}$	Parity $\mathbf{r_2}$	np_s	np_p
III	11111 11111	00100 01000	01000 10100	4	2
IV	11111 11111	01000 01100	00110 00000	4	0

The right-hand curves in Fig. 7 compare the BLER performance obtained with puncturing masks III and IV. The performance gap between the two codes is ~ 0.8 dB at BLER $= 10^{-7}$. Similarly to the binary case, the best asymptotic performance is obtained with the mask yielding the largest value of np_p.

VII. CONCLUSION

We have introduced new design criteria for TC interleavers related to the nature and number of short correlation cycles. It was shown that interleavers optimized via the proposed criteria lead to an improved asymptotic performance of the TC. Furthermore, for high coding rates, we showed that the maximization of the number of non-punctured parity symbols in minimum correlation cycles allows the asymptotic performance of the TC to get closer to its truncated union bound.

ACKNOWLEDGMENT

REFERENCES

[1] R. Garzón Bohórquez, C. Abdel Nour, and C. Douillard, "Protograph-based interleavers for punctured turbo codes," *IEEE Trans. Commun.*, vol. 66, no. 5, pp. 1833–1844, May 2018.

[2] J. Hokfelt, O. Edfors, and T. Maseng, "Turbo codes: correlated extrinsic information and its impact on iterative decoding performance," in *Proc. IEEE 49th VTC 1999-Spring*, vol. 3, Houston, TX, USA, May 1999, pp. 1871–1875 vol.3.

[3] H. R. Sadjadpour, M. Salehi, N. Sloane, and G. Nebe, "Interleaver design for short block length turbo codes," in *IEEE ICC 2000*, vol. 2, New Orleans, LA, USA, June 2000, pp. 628–632.

[4] Y. Saouter, "Selection procedure of turbocode parameters by combinatorial optimization," in *Proc. 6th ISTC*, Brest, France, Sept. 2010, pp. 156–160.

[5] J. Sun and O. Takeshita, "Interleavers for turbo codes using permutation polynomials over integer rings," *IEEE Trans. Inf. Theory*, vol. 51, no. 1, pp. 101–119, Jan. 2005.

[6] ETSI, "LTE Evolved Universal Terrestrial Radio Access(E-UTRA): Multiplexing and channel coding," TS 136 212 (V10.0.0), January 2011.

[7] S. Crozier and P. Guinand, "Distance upper bounds and true minimum distance results for turbo-codes designed with DRP interleavers," *Annals of Telecommunications*, vol. 60, no. 1-2, pp. 10–28, 2005.

[8] C. Berrou, Y. Saouter, C. Douillard, S. Kerouedan, and M. Jezequel, "Designing good permutations for turbo codes: towards a single model," in *Proc. IEEE ICC'04* , vol. 1, Paris, France, June 2004, pp. 341–345.

[9] ETSI, "Digital Video Broadcasting (DVB): interaction channel for satellite distribution systems," EN 301 790 (V1.3.1), March 2003.

[10] ——, "Digital Video Broadcasting (DVB): second generation DVB interactive satellite system (DVB-RCS2): Part 2: Lower layers for satellite standard," EN 301 545-2 (V1.1.1), January 2012.

[11] IEEE, "IEEE standard for local and metropolitan area networks, Part 16: Air interface for fixed and mobile broadband wireless access systems," IEEE Std 802.16-2004/Cor 1-2005, Feb. 2006.

[12] R. Garzón Bohórquez, C. Abdel Nour, and C. Douillard, "On the equivalence of interleavers for turbo codes," *IEEE Wireless Commun. Lett.*, vol. 4, no. 1, pp. 58–61, Feb. 2015.

[13] X.-Y. Hu, E. Eleftheriou, and D.-M. Arnold, "Progressive edge-growth tanner graphs," in *Proc. IEEE Global Telecommun. Conf.*, vol. 2, San Antonio, TX, USA, Nov. 2001, pp. 995–1001.

[14] E. Dijkstra, "A note on two problems in connexion with graphs," *Numerische Mathematik*, no. 1, pp. 269–271, 1959.

[15] N. Biggs, "Minimal regular graphs with given girth," in *Algebraic graph theory*. New York, NY, USA: Cambridge University Press, 1974, pp. 180–190.

[16] R. Garzón Bohórquez, C. Abdel Nour, and C. Douillard, "Improving turbo codes for 5G with parity puncture-constrained interleavers," in *Proc. 9th ISTC*, Brest, France, Sept. 2016, pp. 151–155.

[17] S. Crozier, P. Guinand, and A. Hunt, "Estimating the minimum distance of large-block turbo codes using iterative multiple-impulse methods," in *Proc. 4th ISTC*, Munich, Germany, April 2006, pp. 1–6.

[18] R. Klaimi, C. Abdel Nour, C. Douillard, and J. Farah, "Design of low-complexity convolutional codes over GF (q)," *arXiv preprint arXiv:1807.02481*, 2018.